



Using fractal and multifractal methods to reveal geophysical anomalies in Sardouyeh District, Kerman, Iran

Sarina Akbari¹ · Hamidreza Ramazi¹ · Reza Ghezelbash¹

Received: 17 January 2023 / Accepted: 25 April 2023 / Published online: 17 May 2023
© The Author(s), under exclusive licence to Springer-Verlag GmbH Germany, part of Springer Nature 2023

Abstract

In recent decades, airborne geophysical technologies have gained popularity in mineral prospecting, especially at regional scales with limited rock outcrops and intricate geological conditions dominating the region, that impose errors to the obtained results. To address this, incorporation of fractal/multifractal methodologies into geophysical data will result in more certain outcomes. In this research, content-area (C-A), multifractal inverse distance weighting (MIDW) and singularity index (SI) methods were applied on airborne magnetometric and radiometric data to discover favorable copper mineralization areas in Sardouyeh district, SE Iran. Based on success-rate curves, MIDW and C-A fractal methods had far better performance in highlighting the main anomalies than ordinary IDW. However, they could not separate local anomalies. In contrast, the singularity mapping as a windows-based technique provided more optimal results, which, in addition to the main anomalies, could highlight the weak and local geophysical anomalies dominated by the strong background. Accordingly, the newly revealed anomalies using singularity technique are strongly correlated to the known copper deposits and geological evidences in the region. Moreover, to more accurately determine the geophysical anomalies spatially linked to Cu deposits and generate 2-class (favorable/non-favorable) singularity maps, the normalized density index was implemented. The results demonstrated that α values of 1.96 and 1.94 are optimal thresholds for mapping singularity values of magnetometric and radiometric anomalies, respectively. Therefore, the favorable classes derived by normalized density index are suggested to be used for tracing undiscovered Cu deposits in further exploration stages.

Keywords Geophysics · Aeromagnetic · Radiometry · Multifractal · C-A fractal · Singularity

Introduction

Airborne geophysical methods have received much attention in regional-scale mineral exploration, especially in places where outcrop of rocks related to mineralization are limited (Valenta et al. 1992). These methods are able to cover a large area in a short time with high accuracy that will save time and decrease huge costs of exploration (Karim and Mohamed 2008; Gunn and Dentith 1997; Betts et al. 2003; Gonçalves and Sampaio 2013; Ali et al. 2017; Zhang et al. 2022). In other words, these types of geophysical surveys complete traditional mineral mapping

and enhance field geological observations (Karim and Mohamed 2008). This research intends to concentrate on aeromagnetic and radiometric data which are commonly used as geo-database for geological interpretations, mineral exploration and detection of structural and geological processes such as faults, shear zones, intrusions and folds (e.g. Telford et al. 1976; Cordell and Grauch 1985; Miller and Singh 1994; Edwards et al. 1998; Fedi and Florio 2001; Cooper 2003; Verduzco et al. 2004; Wijns et al. 2005; Uwiduhaye et al. 2018; Liu et al. 2021). Moreover, their resultant anomalies can be effectively used in further advanced researches especially, GIS-based mineral prospectivity mapping (Bonham-Carter 1994; Carranza 2009; Wang et al. 2012; Abedi et al. 2012; Forson et al. 2021; Akbari and Ramazi 2023). The most important aspect of using aeromagnetic and radiometric data is to separate their anomalous contents from the background values (Bai et al. 2010). There are various techniques used frequently for this purpose, which vary from simple statistical methods (based on statistical parameters of the distribution function)

Communicated by H. Babaie

✉ Hamidreza Ramazi
ramazi@aut.ac.ir

¹ Faculty of Mining Engineering, Amirkabir University of Technology, Tehran, Iran

to complex fractal and multifractal methods (based on the spatial structure of the data) (Cheng et al. 1994). Statistical techniques only separate anomalous classes in a traditional way in which spatial distribution and autocorrelation structure of data are not considered. However, geostatistical interpolation models are able to analyze spatial structures with considering their spatial features in the process of interpolating and identifying trends. But the main problem with such interpolation methods is that they smooth out the anomalies, which means that weak anomalies may not be seen or may overlap with high background values. This is a critical problem that is much more common in mineral prospectivity mapping within complex geological media that may cause missing a number of important exploration targets (Cheng 2007; Chen et al. 2018). By contrast, fractal and multifractal methods take into account the spatial distribution of data as well as the geometric shape of the anomalies. Also they use all data without changing them, so they are much more efficient for accurately separating anomaly and background classes (Carranza 2008; Ghezelbash and Maghsoudi 2018a; Kalantari et al. 2020). The Content-Area fractal, singularity index and multifractal IDW are some of powerful fractal and multifractal techniques that not only consider the fractal characteristics of the data but also have a great ability to detect anomalies within complex geological media by reducing the background effect (Cheng and Agterberg 2009; Cheng et al. 2010; Yuan et al. 2015; Agterberg 2012; Bai et al. 2010; Cheng 2007, 2012; Liu et al. 2013; Sun and Barros 2010; Sun et al. 2016; Wang et al. 2013; Xiao et al. 2012; Zhao et al. 2016; Ghezelbash et al. 2019c). Despite the fact that fractal and multifractal methods have been used in many geochemical studies to separate anomalous populations based on geochemical data (e.g., stream sediment, lithochemical, and etc.), they haven't been used much to separate geophysical anomalies, especially regional airborne geophysical data. (Ferdows and Ramazi 2015a, 2015b, 2016; Akbari et al. 2020). So, the main novelty aspect of this paper is to use different fractal and multifractal models for separation of geophysical anomalies linked to aeromagnetic and radiometric data collected from Sardouyeh area, Kerman province, Iran.

The main purpose of this study is to apply Content-Area fractal, singularity index and multifractal IDW as robust separation techniques and compare their efficiency using success-rate curves in order to identify Cu mineralization prospective areas (mostly porphyry and skarn systems) aiming at introducing new exploration targets. The quantitative assessment of geophysical anomalies (both aeromagnetic and radiometric) derived from Singularity Index technique was carried out using an authentic metrics namely normalized density index (N_d) (Ghezelbash et al. 2018b).

Study area and data used

Sardouyeh area

The study area) 1:100,000 scale Sardouyeh quadrangle map) is located in Kerman province, southeastern Iran (Fig. 1). The Sardouyeh district is situated in the southwestern part of the 1:250,000 scale Bam geological map and includes four 1:50,000 scale sheets called Gishigan Bala, Farash, Deh Seyed Morteza and Sarmashk.

The coordinates of the area are between east latitude $57^{\circ} 00'$ to $57^{\circ} 30'$ E and north latitude $29^{\circ} 00'$ to $29^{\circ} 30'$ N. From the structural point of view, the study area is placed within the Urmia-Dokhtar magmatic belt (UDMB), which extends in the northwest-southeast direction and along the Zagros Trust fault with a length of more than 2000 km. Copper mineralization is very numerous in the region and it hosts the most important and world-class porphyry Cu deposits in Iran, especially Soorakhmar, Bondarhanza and Daraloo porphyry Cu deposits. Vein-type mineralization are mainly present in Eocene volcanic structures and along highly silicified faults. This mineralization mostly includes chalcopyrite, pyrite, bornite and magnetite (Sabzehie and Afrooz 1990).

Geological settings

The lithology of Sardouyeh region in terms of geological time includes the Colored M \acute{e} lange ensemble of upper Cretaceous as the oldest outcropping units, appears only in the southwest corner of the study area. It is mainly composed of mafic rocks (spilites and their pyroclastics, diabases and serpentinites), with red chert and limestone blocks and lumps. The Eocene formations (mostly in the northern and middle parts) can be divided into two complexes which are overlaid by the sedimentary volcanic complex and form a large part of the area with a thickness of about 7 km. Its lithology ranges from andesite-basalt to andesite and related pyroclastics are along with limestone, conglomerate and sandstone. In the upper parts, there is a pyroclastic unit with a thickness of more than 700 m with lava flows, trachyandesite-basalt and trachyandesite. Rhyolite agglomerates, tuffs, shear tuffs, and lava sections followed by andesitic and rhyolitic flows form the lowest exposed unit of this complex in the northern part of the study area. The upper part of the Middle Eocene is composed of rhyolite tuffs and tuffaceous sandstones, silt, marl and conglomerate. The rock units of the Eocene age have been infiltrated by intrusions composed of trachyandesite. Large intrusions of granite and granodiorite form the main trunks of the Hanza and Bahr Asem \acute{a} n Mts. and occur also as smaller bodies throughout the area. Andesite-basalt and andesite lava flows are

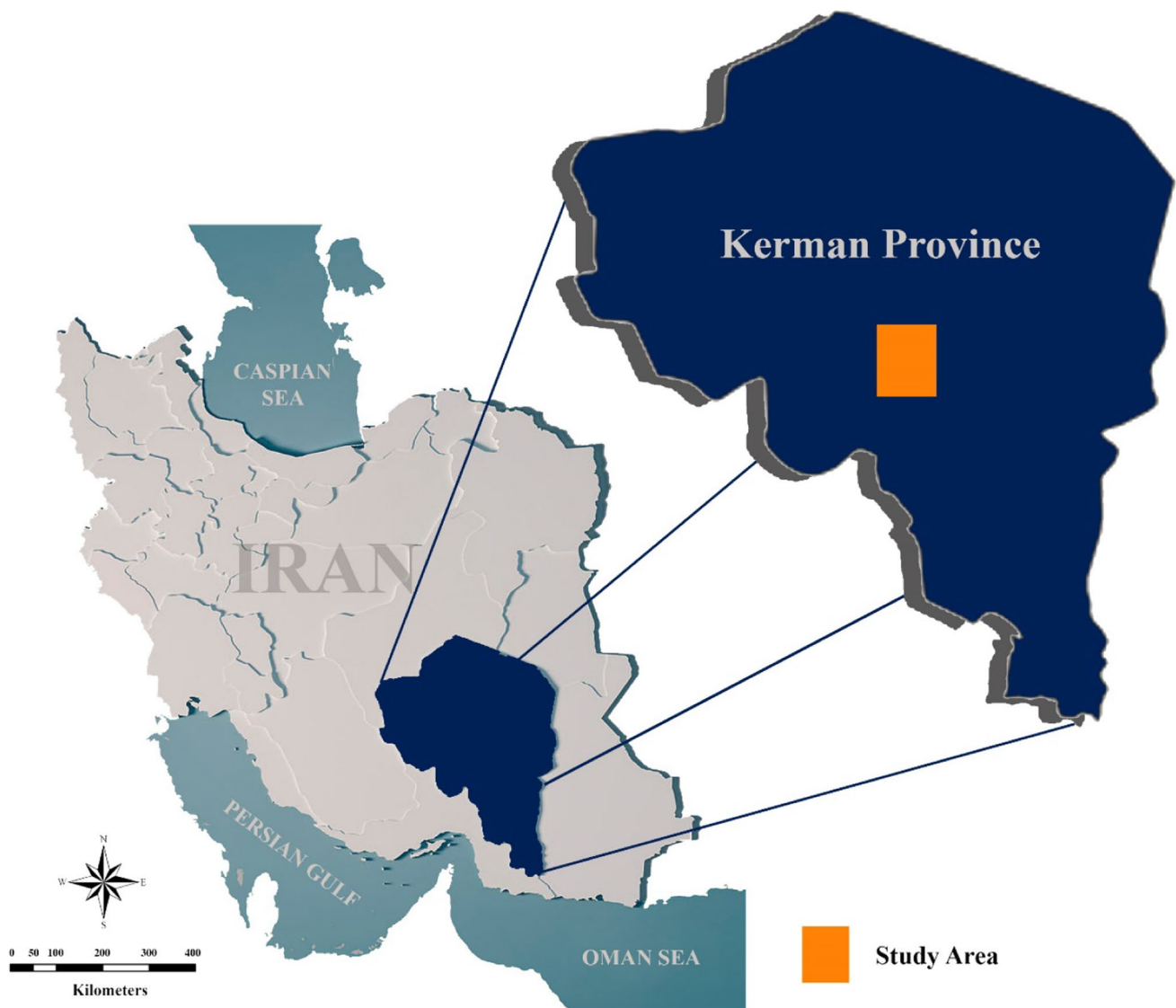


Fig. 1 Location of the study area on the map of Iran

appeared sparsely in the lower part of this unit, but they form a conspicuous unit at the top of it. The lava flows are accompanied by agglomerates and tuffs. There is a slight discontinuity on this conspicuous unit that represents the Oligomycin. Turbidite sediments are also observed. The basal part of the Oligocene–Miocene sediments is represented by a few decameters of conglomerates. Upwards they develop into monotonous yellow silt-grained biosparites, in places marly biomicrites with pseudo-ooliths, dolomitic limestones, and sandy marls. Younger Neogene sediments cover rather small areas, being represented by a poorly lithified conglomerate with some sandstones. Quaternary sediments are represented by older and younger gravel fans,

calcareous terraces, talus cones, clay flat and recent alluviums (Sabzehie and Afrooz 1990) (Fig. 2).

In terms of economic geology, the predominant mineralization in this area is copper, which is directly associated with diorite to granodiorite intrusive rocks of post Eocene. Copper ore deposits/occurrences are widely distributed throughout the study area, most of which are genetically and spatially linked to porphyry systems. Mineralized veins, mostly in Eocene volcanics, are formed along the highly silicified faults. The Cu mineralization is appeared as filling within fractures and does not show a relationship with metasomatic substitutions. They are mineralized by chalcopyrite, pyrite, bornite and magnetite (Sabzehie and Afrooz 1990).

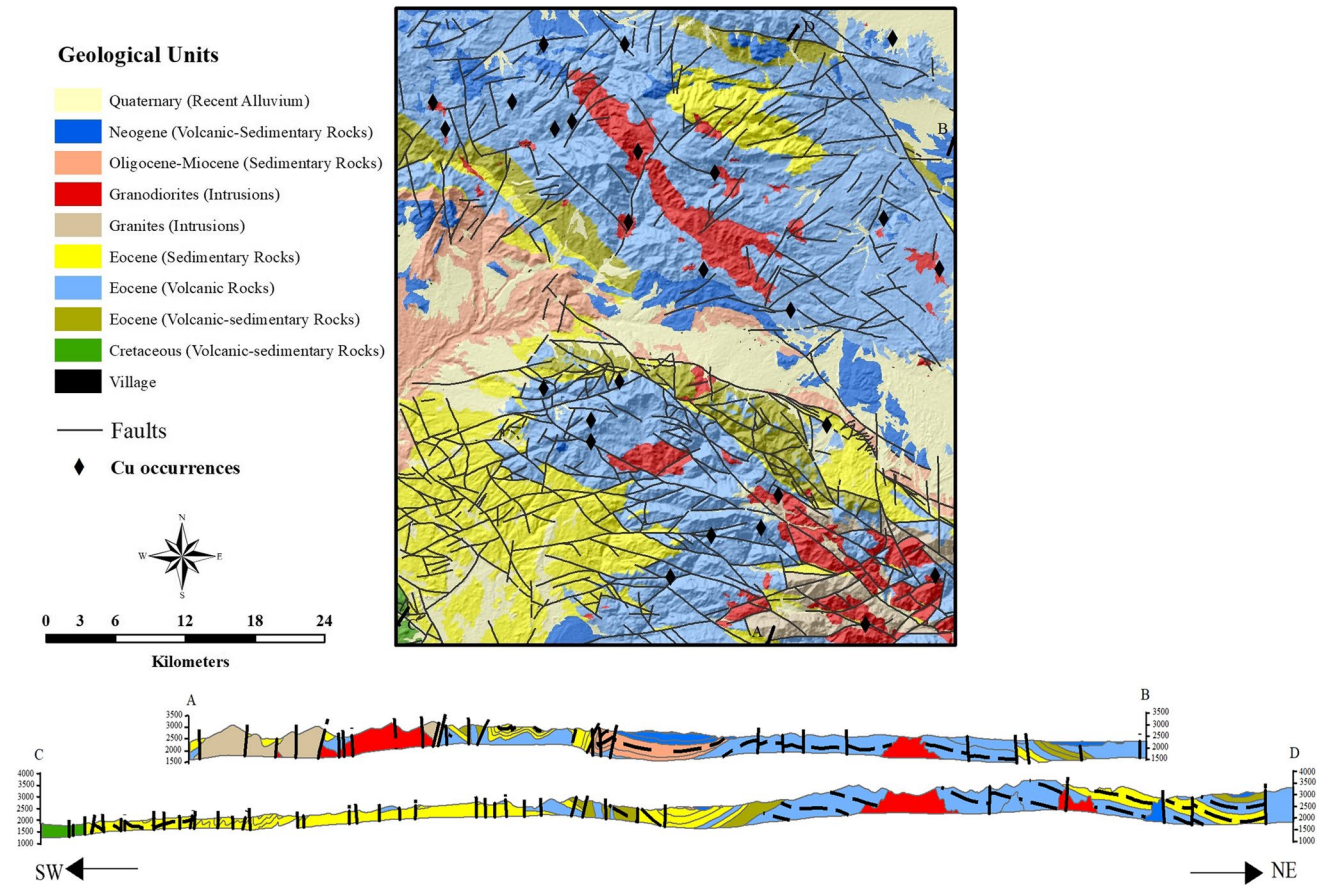


Fig. 2 Simplified geological map of the 1:100,000 scale Sardouyeh district

Geophysical dataset

The geophysical data used in this study (airborne magnetic and radiometric data), were collected in a regular network with north–south trending flight lines and a distance of 1 km from each other using a Cesium vapor magnetometer. The flight altitude was 120 m above sea level and the aircraft speed was between 80–100 km per hour and 10 readings had been performed continuously every second. In total, 68,108 points have been measured in this area with a distance of about 200 m between the measured points.

Methods

Reduction-to-pole (RTP)

When using a magnetic field, the shape of anomalies is heavily influenced by inclination and declination of geomagnetic field that has only vertical effects at the north and south magnetic poles. In other locations, the maximum value of magnetic field is not atop the sources that are actually causing it. Due to this characteristic, interpreting magnetic anomalies is

often challenging (Wang and Meng 2019). In this research, RTP which first proposed by Baranov (1957) was applied at an inclination of 44.6° and a declination of 1.86° using Geosoft Oasis Montaj 8.4 software. Figure 3 shows the Total magnetic intensity (TMI) map and reduced-to-pole magnetic map of the study area. It should be noted that all further processing is done on the RTP map.

Multifractal inverse distance weighted (MIDW) method

One of the most common geoprocessing tools for data interpolation tasks is inverse distance weighting available in ArcGIS software (Bartier and Keller 1996). IDW is a moving average technique in which the interpolation is more influenced by neighbor observation values than distant observation values (Cheng 2008). Even though this technique is often used to find spatial variations and anomalies by making contours and surfaces, it always smooths out the data (Cheng 2001; Zuo and Wang 2016). So, it can't successfully reproduce every outlying data during the interpolation. In other words, it doesn't considerate the local properties of the data which is the most common bug of moving average

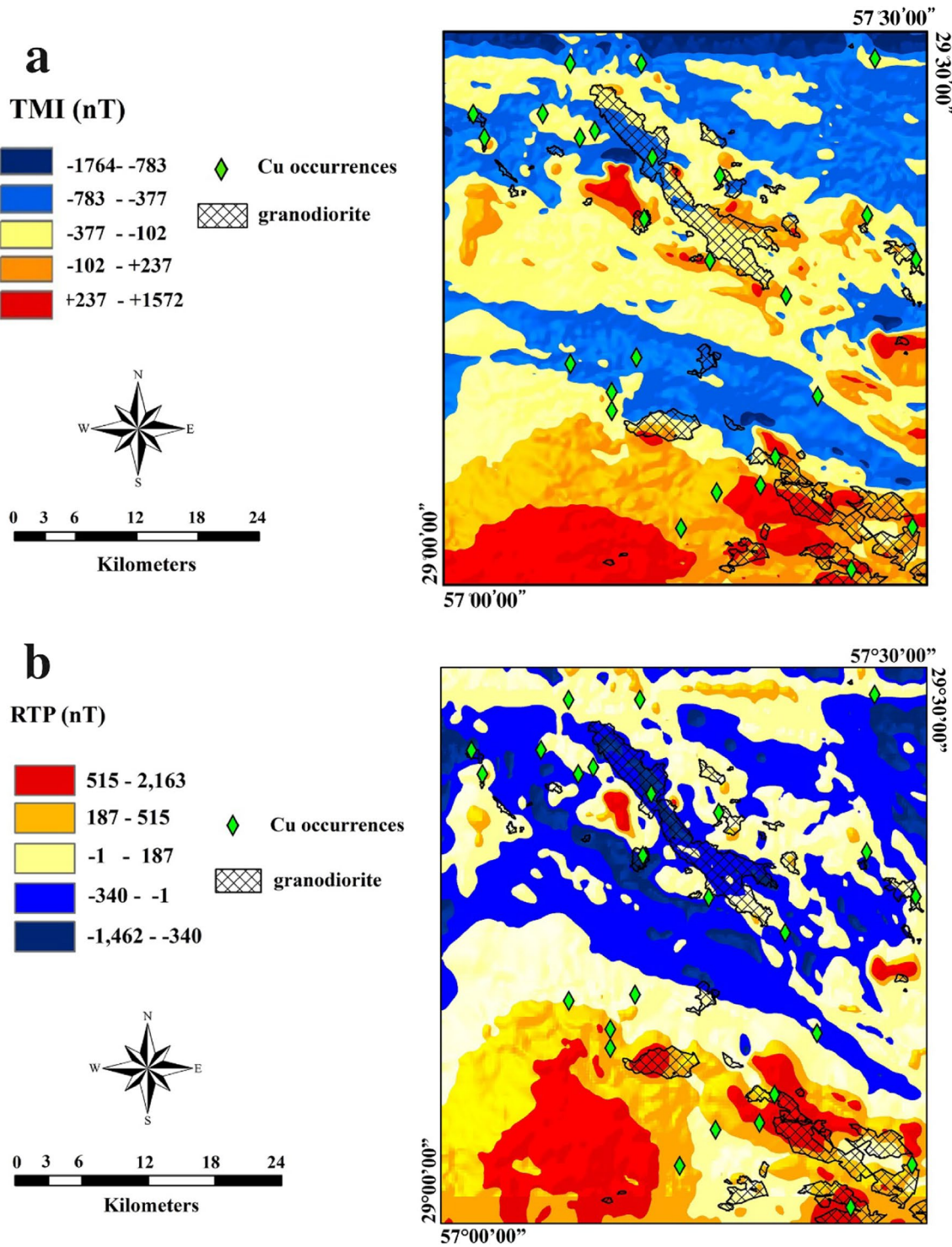


Fig. 3 (a) Total magnetic intensity map and (b) reduced-to-pole magnetic map of the study area

interpolation techniques (Chen et al. 2018). Hence, to overcome the shortcomings of the ordinary inverse distance weighting method, the multifractal inverse distance weighting model was proposed by Cheng (1999), in which the spatial correlation between data, local structures, and the local

singularity values are simultaneously considered. In other words, this technique can precisely coordinate the source data and retain local anomalies during the interpolation. This is helpful for separating anomalies from background by using fractal filtering especially in complex problems

(Lima et al. 2003). In general, the multifractal inverse distance weighting model has two fundamental advantages over the ordinary interpolation method (e.g., IDW): (1) improving the validity of the interpolation outcome and (2) preserving the local structures and interpolation variances as well as displaying the primary high and low values (Cheng 1999, 2000; Ghezelbash et al. 2019a).

The moving average relation of the MIDW technique has been described by Cheng (2000) as follows:

$$\rho(\varepsilon_1) = \varepsilon_1^{\alpha(x_0)-2} \sum_{\Omega(x_0,1)} \omega(\|x_0 - x\|)Z(x) \quad (1)$$

where $\Omega(x_0,1)$ is the window size, ω is the weight of moving average function and $\alpha(x_0)$ is the value of local singularity index at the location of x_0 . According to this equation, it can be seen that the MIDW method is able to consider the singularity values in addition to considering spatial relationships. In this relation, when the $\alpha(x_0)$ is equal to 2, x is located in the background field and there is no singularity and hence, the results of this method are the same as other weighted average methods. However, if x_0 is located in a place with high values (i.e., areas of enrichment) and the α value is less than 2 ($\alpha(x_0) < 2$), the results of this method will be more than ordinary weighted average methods. Likewise, when $\alpha(x_0) > 2$ and x_0 is located on low values (i.e., areas of depletion), the result of the method is usually lower than the ordinary weighted average results.

C-A fractal method

One of the most critical issues in geochemical exploration studies, is to determine and separate anomaly contents from the background (Bai et al. 2010). There are extensive techniques for this purpose, including content-area (C-A) fractal method which was proposed by Cheng et al (1994) for separating geochemical anomalies (e.g., Ghezelbash and Maghsoudi 2018a; Ghezelbash et al. 2018b), while the concept of fractal geometry was firstly introduced by Mandelbrot (1983) to describe the self-similar phenomena. The C-A fractal method is based on the amount of area occupied by each specific concentration (or content) in that area. As the concentration (or content) of an element increases, the amount of occupied area decreases. This approach can identify anomalous populations and different degrees and intensities of anomaly (Cheng et al. 1994; Carranza 2009). The fractal distribution of components in nature is what gives it this capacity (Goncalves et al. 2001).

In addition to geochemical studies, the fractal method is useful in other branches of earth science, including geophysics (Ferdows and Ramazi 2015b; Akbari et al. 2020) and tectonics. In general, geophysical data have the same multifractal behavior as geochemical data. This shows how

much geological, geochemical, alteration, surface weathering, mineralization, and thus enrichment of an element change (Goncalves et al. 2001). As mentioned in the previous section, in the similar studies for interpretation of the magnetometric data, it is necessary to apply the RTP filter to the data before any operation (Baranov and Naudy 1964; Guan 2005; William et al. 2013). In the RTP map, due to the transfer of the abnormality location to the magnetic pole, where the earth's magnetic field becomes vertical, the effect of the geographical situation, i.e., inclination and deviation angles, is removed. This processing causes the location of the magnetic anomaly to be corrected relative to the mineralization place. In fact, the magnetic anomaly is placed above the deposit location. Therefore, the results are more accurate and closer to reality and thus, fractal and multifractal approaches should apply on RTP map.

One of the most typical ways to show the content distribution of an element in an area is to draw a contour map of the equivalent element. If the value of each contour is considered equal to ρ , a power equation can be presented as follows for the content of materials with fractal characteristics (Cheng et al. 1994; Carranza 2009):

$$A(\rho \leq v) \propto \rho^{-a_1}; A(\rho > v) \propto \rho^{-a_2} \quad (2)$$

where α shows proportion, $A(\rho)$ is the occupied area with content values greater than contour values ρ , a_1 and a_2 are the fractal dimensions of anomaly and background populations, respectively and v shows the threshold value.

Cheng et al (1994) had proposed two approaches to achieve this goal:

- (1) Measuring the vicinity surrounded via the contour value ρ on a contour map;
- (2) Numeration of pixels greater than or equal to v (the so-called box-counting technique).

For this purpose, a log–log plot of the cumulative frequency (ρ) versus the occupied area, $A(\rho)$, is drawn (Ghezelbash and Maghsoudi 2018b). The logarithmic plot of contents against areas breaks at some points and changes in the slope of this plot indicating a shift from background to anomaly (Agterberg et al. 1996). Threshold values are extracted from these points to put gridded values into proper anomaly and background classes.

Singularity mapping technique

Singularity methodology (Carranza et al. 2012) is one of the most prominent multifractal modeling methods. It is defined by anomalous behavior of singular physical processes that release abnormal amounts of energy or accumulate material within a limited spatial–temporal interval (Cheng 2007,

2008, 2012; Cheng and Agterberg 2009). This concept has been used in various sciences to describe singular natural phenomena including climate research, natural hazards and thus, multifractal phenomena. Accordingly, geochemical and geophysical data can be modeled using this technique. Singularity is an important tool for detecting local enrichment and depletion in two-dimensional maps. In fact, Singularity Index method which first proposed by Cheng (2007), is a moving window method based on the multifractal relationship between metal density and its surrounded area. The singularity can be estimated using the following equation:

$$X = c.r^{\alpha-E} \quad (3)$$

where X is the elemental contents, c is a constant value, r is the cell size, α is the singularity value in every location and E is the Euclidian dimension (Cheng 2007). In this method, two types of weak and strong anomalies linked to geophysical data are identified using MATLAB software. To this end, the following steps should be performed:

- 1) A position on the map is considered with a number of variable windows $A(r)$ (square) $r_{\min} = r_1 < r_2 < \dots < r_n = r_{\max}$ and the average content of $C[A(r_i)]$ is calculated for each window size on the map.
- 2) Eq. 3 is used to implement the data ($i = 1, \dots, n$) $C[A(r_i)]$ and r_i in a logarithmic diagram (Wang and Zuo 2018):

$$\log C[A(r_i)] = C + (2 - \alpha)\log(r) \quad (4)$$

The value of $\alpha-2$ can be obtained from the slope of a straight line.

- 3) Repeating the mentioned methods for all parts of the geophysical map.

For a geophysical map, most of the areas are linked to a singularity value (α) close to 2, representing a normal background, whereas the areas with $\alpha < 2$ or $\alpha > 2$ represent an enriched pattern and a depleted pattern of geophysical contents, respectively (Cheng 2007; Ferdows and Ramazi 2015a).

Results and discussion

IDW and MIDW interpolation

In this study, at first, the ordinary interpolation method (here, IDW) was applied to airborne magnetometric and radiometric data. In this method, the estimation is done based on the values of points close to the estimated point, which are weighted according to the inverse distance (Guo et al. 2008; José-Ma & Beatriz 2006; Wu 2005). Figure 4a, b

shows reduced-to-pole Magnetic and potassium-based IDW interpolation results using ArcGIS 10.8 software. According to the Fig. 4a, the magnetic anomaly is mostly appeared in the central, eastern and southeastern part of the area, which is geologically somewhat consistent with the granodiorite outcrops as the main Cu-related rock units in the area referring to Sabzehie and Afrooz (1990). Positive anomalies in these areas can be caused by alteration of mafic minerals to magnetite or the presence of primary magnetite in the ore solution in potassic or propylitic alteration. In the southwestern part of the region, a strong magnetic anomaly is observed, which is not justified in terms of geology and locations of Cu deposits occurrences in the region. This anomaly does not seem to be connected to Cu mineralization. The cause of magnetic depletion at the site of some copper mineralization in the region could be due to a decrease in the magnetite properties because of the hydrothermal alteration such as phyllic or concealment of porphyry systems under thick covers of younger lithological units. The radiometric map shows a potassium anomaly in the north, northeast and a crescent-shaped anomaly in the south. Since this map shows an acceptable correlation with copper deposits occurrences in the region, the anomalies are probably related to potassium alteration located within the center of the porphyry copper systems (Fig. 4b).

To address the problems arise from the ordinary interpolation methods such as IDW, the MIDW method is applied to produce airborne magnetometric and radiometric maps utilizing MATLAB software. As shown in Fig. 6a, b, the MIDW approach can clearly highlight the primary high values and, to some extent, reduce the background effect. By this method, the main anomalies are more outstanding and have a clearer border with the background (Fig 5).

Fractal-based discretization of geophysical layers

As mentioned earlier, the C-A fractal model has been commonly employed to classify geochemical populations and relatively less for geophysical investigations, especially for airborne magnetometric and radiometric data (Cheng et al. 1994). However, using this method to separate geophysical anomaly from background may result in a breakthrough in geophysical interpretations. The log–log plots of C-A fractal models which are generated using Microsoft Excel 2019 software to determine the meaningful threshold values separating the corresponding classes of geophysical layers are demonstrated in Fig. 6. In this plots, the horizontal axis indicates the magnetic or radiometric values of gridded geophysical maps while, the vertical axis shows the occupied area of matching cell values (Fig. 6). The break points represent the transition from one population to another in a way that allows for separating background and anomalies with different intensities (Li et al. 2003).

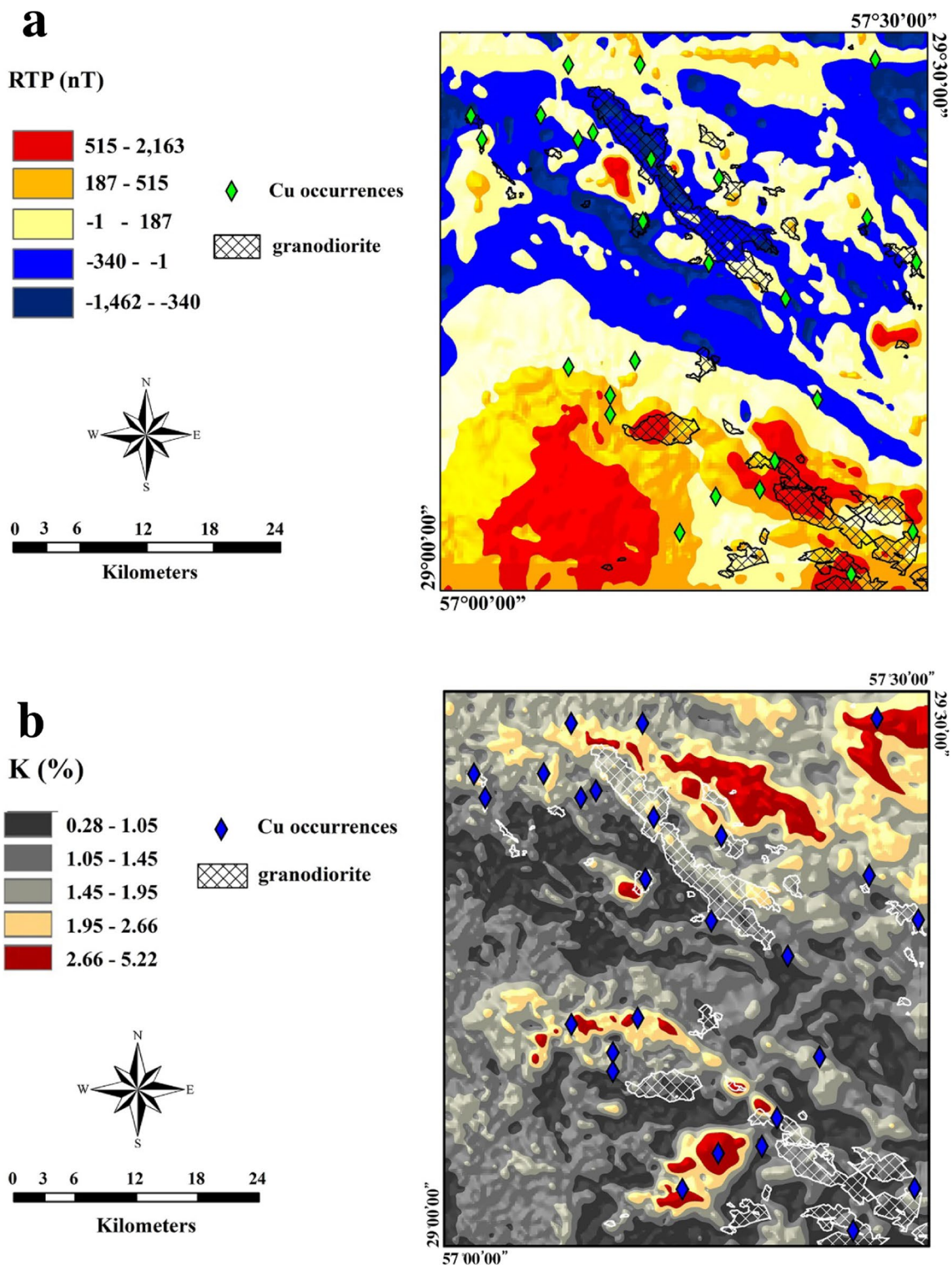


Fig. 4 Geophysical maps constructed by IDW interpolation for (a) magnetometric and (b) radiometric data

According to Fig. 6a, b, there are three different geophysical populations based on two different threshold values for both airborne magnetic and radiometric data that may be related to various lithological units based on their

geophysical characteristics. Using their log–log plots, ArcGIS 10.8 software created classified maps for two types of geophysical data (Fig. 7). The C-A fractal model successfully decomposed various populations. Each distinct class

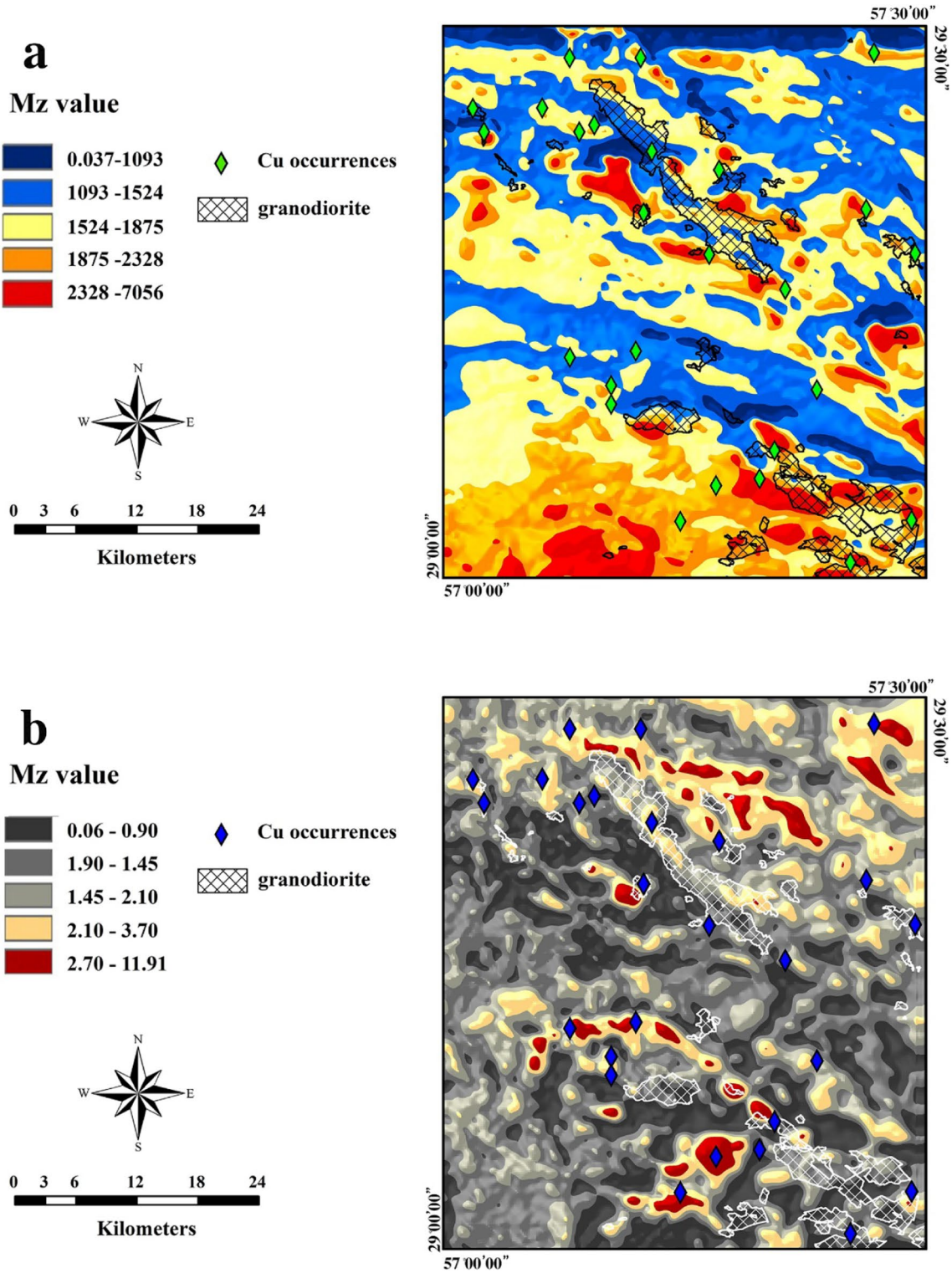
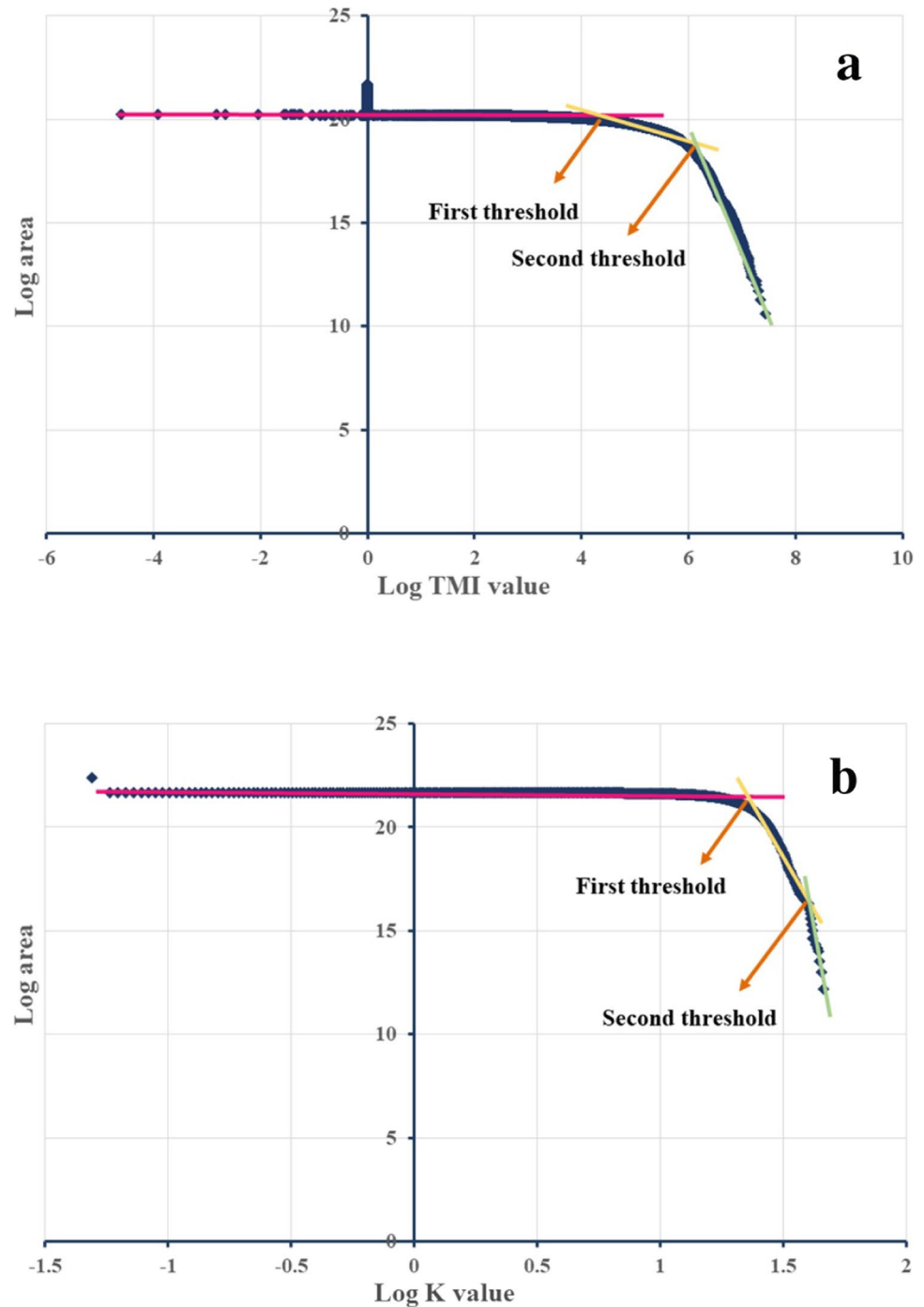


Fig. 5 Geophysical maps constructed by MIDW interpolation for (a) magnetometric and (b) radiometric data

may belong to a specific lithological unit, mineralization system or an alteration zone. As mentioned, the raster to point of airborne magnetic values come in three different groups. The background population which is represented

by the dark blue color, while the moderate and strong magnetic anomalies are represented by the yellow and red colors, respectively. According to geological evidences, strong magnetic anomalies (red color) are associated with

Fig. 6 C-A fractal log–log plots of (a) magnetometric and (b) radiometric data



granodiorite intrusions that are related to porphyry copper deposits in the region (Sabzehie and Afrooz 1990), whereas the second class (moderate anomaly) with lower favorability is associated with the host rock with less magnetization due to the presence of alterations and changes caused by mineralization (Fig. 7a).

The raster to point of airborne radiometric data (potassium radioactivity) were also separated into three classes based on the C-A fractal model (Fig. 7b). The dark gray

color indicates places with extremely background radioactivity. In addition, Potassic alteration associated with porphyry copper deposits is likely indicated by higher radiometric values. The red color with the greatest values (strong anomaly) probably represents the center of the porphyry systems, while the yellow color with relatively lower values (moderate anomaly) reflects their margin, which is also compatible with geological evidence in the region.

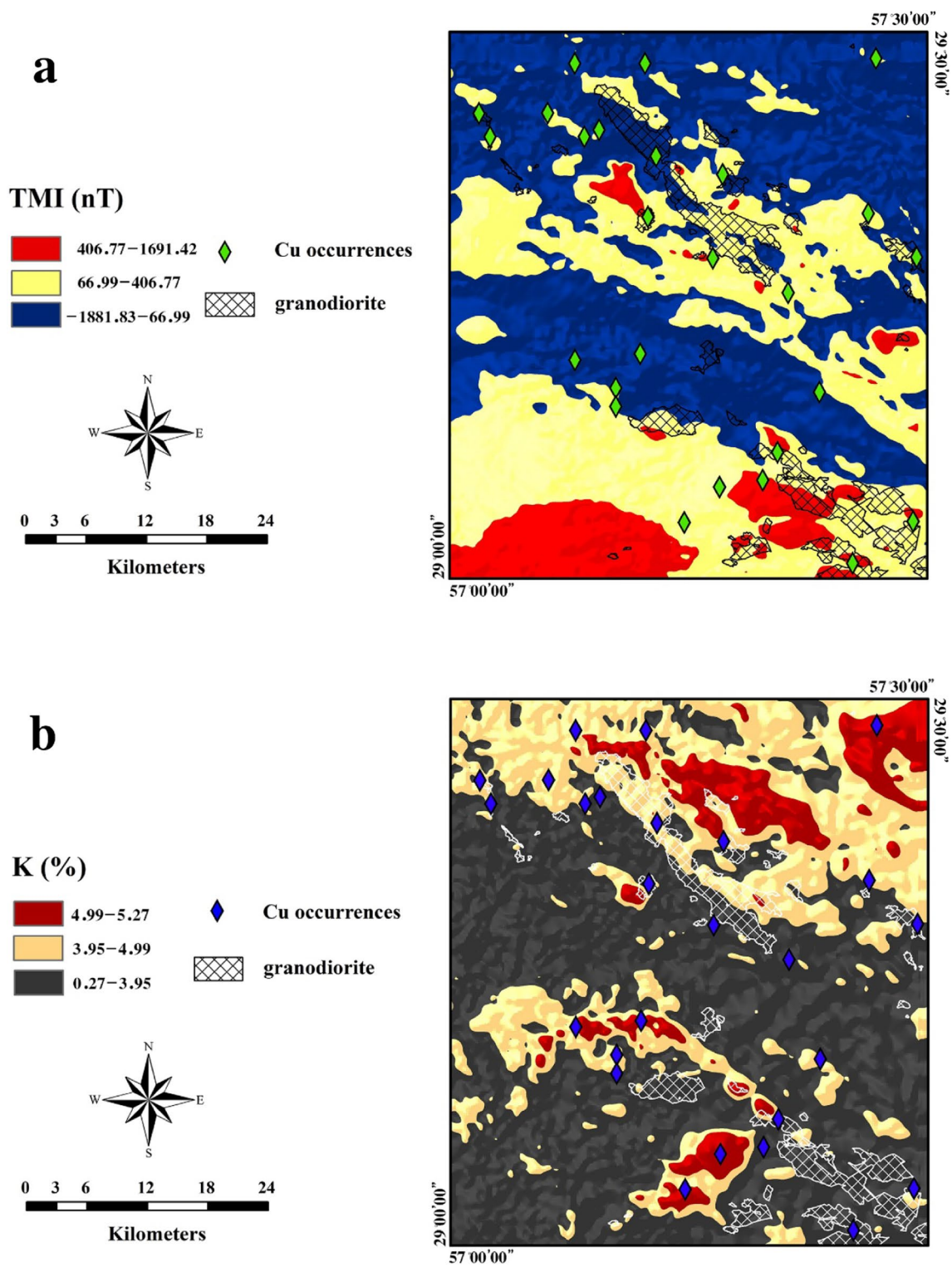


Fig. 7 C-A fractal-based discretized maps of (a) magnetometric and (b) radiometric data

Singularity mapping

Recent developments for identification of weak geochemical anomalies from background refers to singularity

mapping technique suggested by Cheng (2007). This technique has been shown to be an effective multifractal tool for identification of weak geochemical anomalies within complex geological media or overburden-covered

areas. The Singularity index technique frequently develops a multifractal model to identify the spatial distribution of mineralization. Also, it is able to assess the enrichment and depletion of mineralization characteristics. Therefore, in areas with complex and intricate geological conditions, where weak anomalies may conceal within a strong background, the singularity mapping technique is useful for predicting undiscovered mineral resources.

As previously mentioned, the lithological settings of Sardouyeh area is both diverse and complicated. Ordinary IDW, MIDW, and C-A fractal approaches were able to identify strong and major anomalies, but were not useful to detect local and minor anomalies linked to magnetic and radiometric data in the region. Therefore, the singularity method was applied to identify local anomalies related to copper mineralization in this area.

The singularity mapping method was implemented to reduced-to-pole values of airborne magnetic and radiometric data. According to the extent of the study area, the size of the unit cell and the scale of the local structures of interest, the edge sizes and intervals were determined to be employed in singularity mapping. For this purpose, for identifying the local characteristics of geophysical data, a set of six edge sizes with the minimum value of 500 m and the maximum value of 3000 m were used. Using a program which was coded in MATLAB software and considering the proper cell sizes, the average content of each window (α value) was calculated. After calculating the singularity index values for both magnetic and radiometric data, their corresponding maps were generated using ArcGIS 10.8 software (Fig. 8). As visible on the magnetometric map, weak and local anomalies have emerged and are almost spatially associated with known mineral deposits occurrences in the region (Fig. 8a). Some magnetic anomalies have appeared in the northeast and central parts of study area corresponding to the locations of mineral deposits which were not visible in the fractal, Multifractal IDW and ordinary IDW maps. In the radiometric map, the performance of singularity method is clearly obvious (Fig. 8b). Small and local anomalies have revealed throughout the region, and the boundaries between the major anomalies have become increasingly distinct and condensed. Due to the granodiorite units and mineral deposits in the southeast, a strong radiometric anomaly was expected, however the prior radiometric maps showed no potassium anomaly. The local anomalies in mentioned part, which were concealed due to the complexity of the geology, were well revealed using the singularity method. In summary, the results of singularity mapping technique are highly accurate rather than other methods used in this study and consistent with different geological evidences in the study area.

Quantitative evaluation of obtained results using success-rate curve

Comparing performance of the models might be performed using accurate mathematical verification. The success-rate curve, as a reliable validation technique quantitatively measures the modeling accuracy by considering the locations of known mineralization occurrences on anomaly and background populations (Wang and Zuo 2022). In this graph, a diagonal line is used to evaluate the performance of various methodologies. If the success-rate curve of final model is located above the diagonal line, it demonstrates a good spatial correlation between the predictive models and the corresponding mineralization in the study area and vice versa. In fact, this graph can be used to determine model accuracy and technique efficiency (e.g. Rodriguez-Galiano et al. 2015; Sun et al. 2020; Ghezelbash et al. 2019b, 2020, 2022, 2023; Daviran et al. 2021). It also can be used to compare different approaches and choose the best one for further researches (Yang et al. 2021). In this study, the success-rate curve is applied to quantitatively evaluate the performance of geophysical models resulting from techniques employed in this study (Fig. 9). The greater the positive distance of each model's curve from the gauge line, the greater its efficiency and performance. As depicted in the graphs (Fig. 9), for both magnetometric and radiometric data, the success-rate curve derived from the singularity model is significantly higher than the diagonal line and also the curves related to the rest of the three models (Fig. 9a, b). This means that the singularity model could successfully portray prospective areas associated with copper mineralization in Sardouyeh district and has the best performance for revealing the geophysical anomaly signatures. However, the fractal method, MIDW and IDW ranked next in terms of efficiency and performance, respectively. To more accurately determine all regional and local magnetometric and radiometric anomalies derived from SI method which are spatially linked to Cu deposits, the normalized density index (N_d) (Agterberg, and Bonham-Carter 2005), as another reliable validation technique, was implemented. To define how well geophysical anomalies perform, the occupied areas (O_a) and the prediction rates (P_r) of anomaly classes calculated using $N_d = P_r / O_a$. For this purpose, different N_d values were computed based on different α values (2–1.93) to identify optimized thresholds for separating favorable and non-favorable areas. As can be seen in Table 1, $\alpha = 1.96$ was selected as the optimized threshold value ($N_d = 4.12$) for separation of magnetometric favorable anomaly class from non-favorable and generate 2-class favorability map (Fig. 10a). This was also carried out for radiometric data in which $\alpha = 1.94$ was selected as optimized threshold ($N_d = 2.82$) (Table 2) for delineating radiometric 2-class favorability map (Fig. 10b). As shown in Figs. 10a, b, the derived magnetometric and

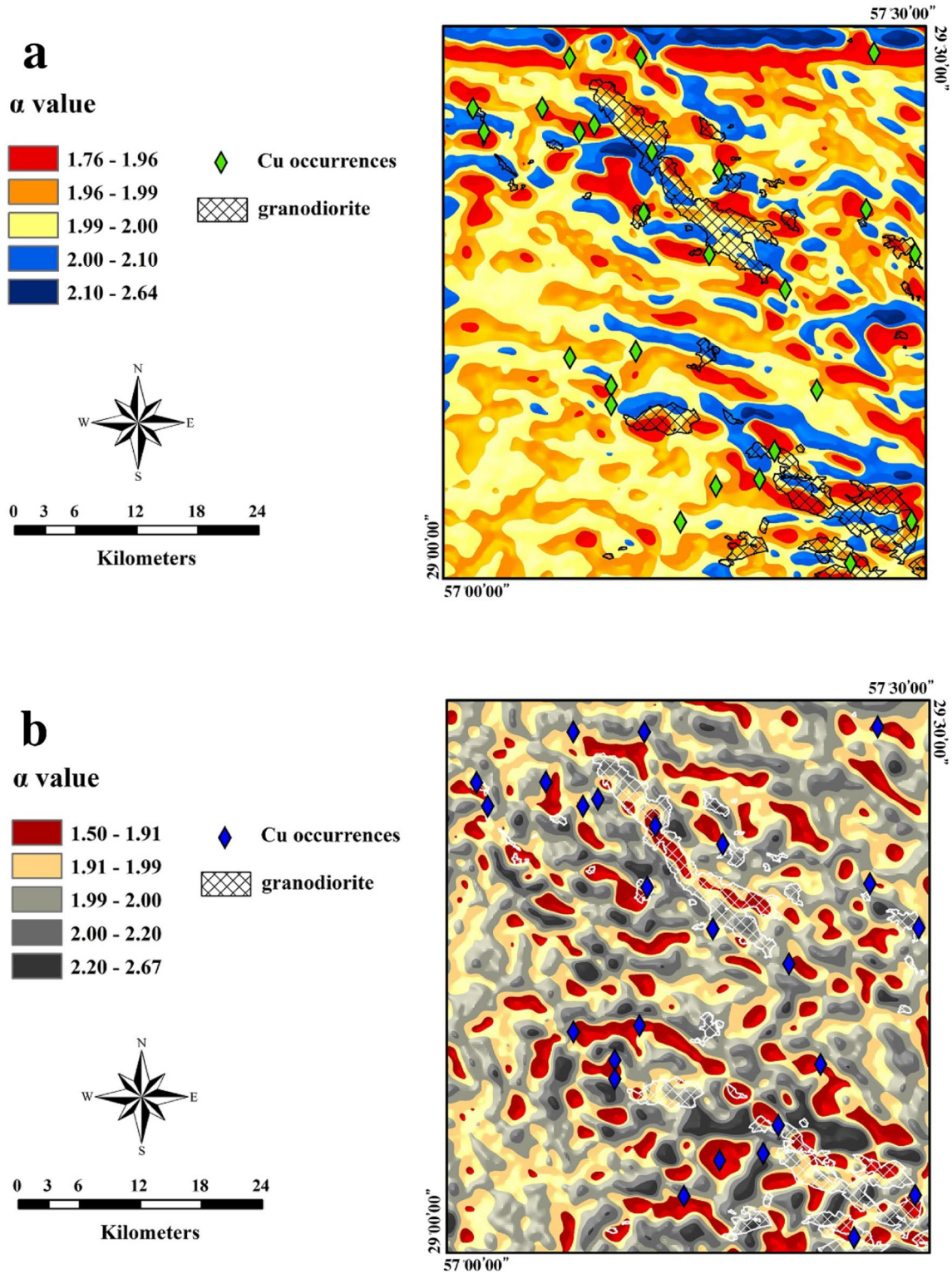
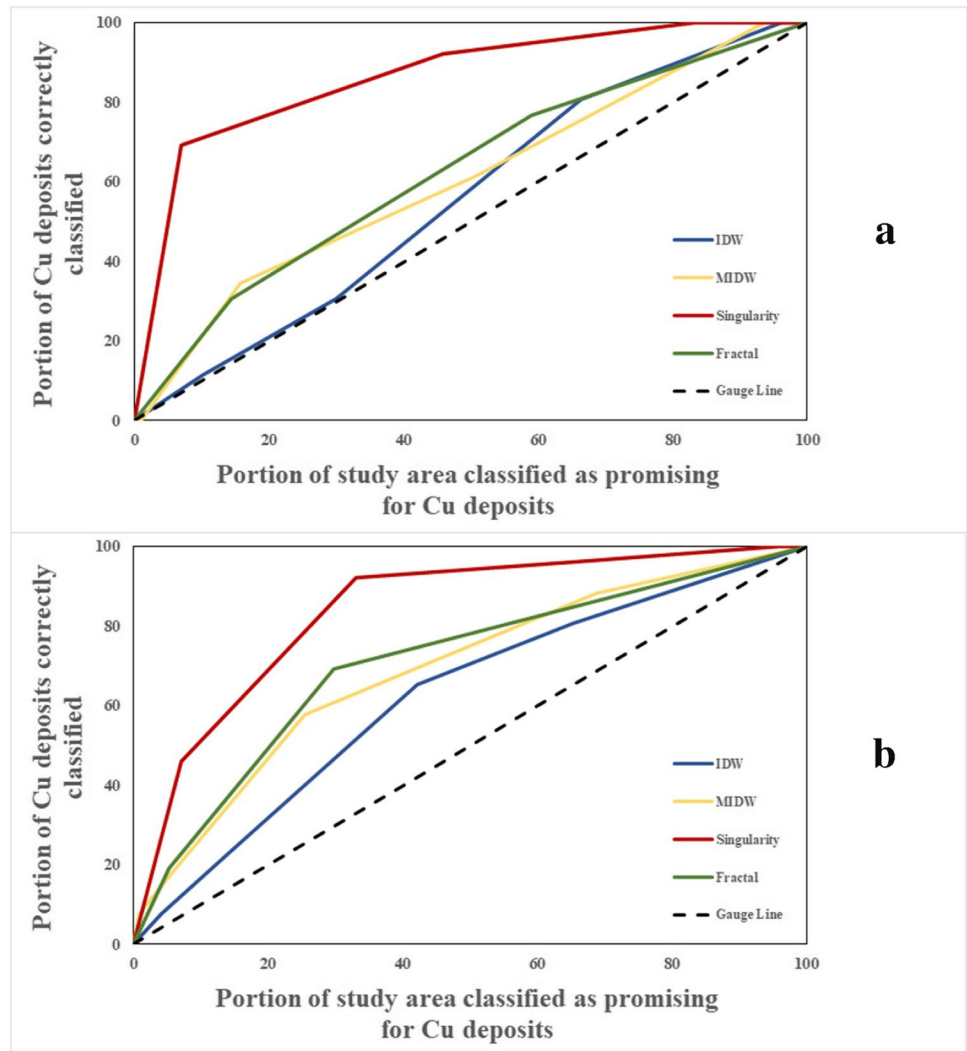


Fig. 8 The spatial distribution map of singularity index for (a) magnetometric and (b) radiometric data

Fig. 9 Success-rate curves of models derived from IDW, MIDW, singularity and fractal approaches



radiometric favorable anomaly classes are strongly associated with known Cu deposits occurrences. Moreover, the regional and local anomaly signatures are geospatially linked to granodiorite intrusion outcrops which make them high prospective for future exploration programs discovering new Cu deposits in this area of investigation.

multifractal inverse distance weighting, and singularity index as powerful fractal and multifractal methods. The obtained results showed that all three strategies were able to improve the responses of geophysical models. Compared to the ordinary IDW, the multifractal IDW method provided better results in both types of geophysical data and revealed

Conclusions

In regional-local scale studies within complicated geological media, using airborne geophysical methods without the help of optimizer methods can cause inaccurate results and concealment of weak and local anomalies by the strong background. To acquire satisfactory findings, it is essential to analyze the geophysical data using more proper methodologies such as fractal and multifractal approaches. In this study, airborne magnetometric and radiometric geophysical data were processed using the Content-Area fractal,

Table 1 Prediction rate (P_r), occupied area (O_a) and normalized density (N_d) of singularity classes for magnetic data

α value threshold	P_r	O_a	N_d
2	0.76	0.46	1.65
1.99	0.73	0.31	2.29
1.98	0.65	0.22	2.94
1.97	0.61	0.16	3.8
1.96	0.5	0.12	4.12
1.95	0.34	0.08	3.86
1.94	0.23	0.06	3.47
1.93	0.19	0.04	3.91

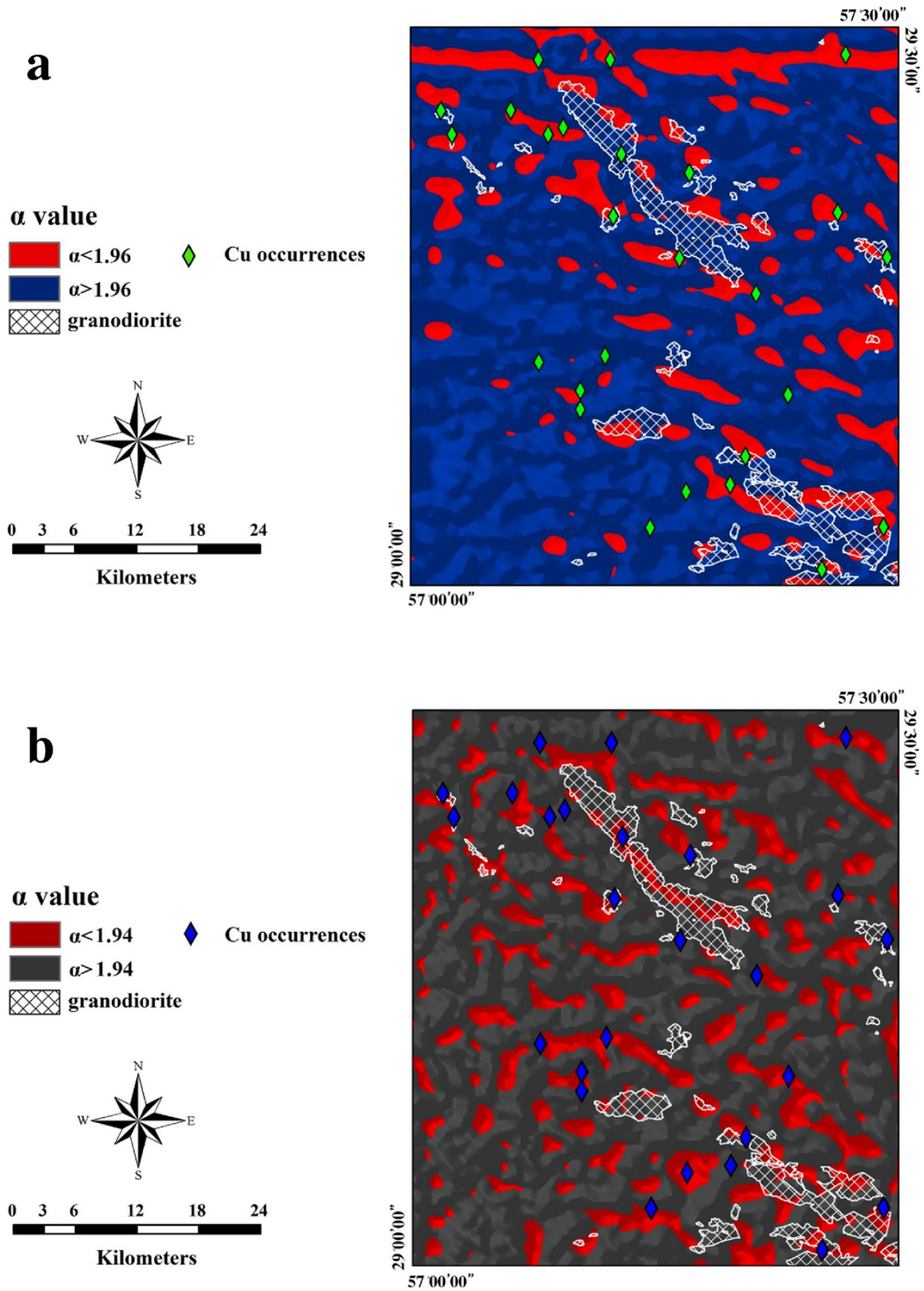


Table 2 Prediction rate (P_r), occupied area (O_a) and normalized density (N_d) of singularity classes for radiometric data

α value threshold	P_r	O_a	N_d
2	0.76	0.46	1.66
1.99	0.76	0.41	1.84
1.98	0.76	0.37	2.06
1.97	0.76	0.32	2.33
1.96	0.73	0.28	2.52
1.95	0.65	0.25	2.6
1.94	0.61	0.21	2.82
1.93	0.57	0.21	2.65

the main anomalies more prominent and dense, but failed to uncover local and weak anomalies. The fractal approach provided relatively better results in identification and discretization of the main anomalous areas, however, it was also unable to detect small and weak anomalies. Finally, the multifractal singularity technique was applied, which provided the most acceptable results. The new weak and local anomalies are well defined in both radiometric and magnetometric maps, the major anomalies are condensed, and the boundaries get sharper. The success-rate curves prepared for different methods also confirmed the findings and the multifractal singularity was considered as the most effective separation method for identification of weak and local anomalies within complex geological settings. In summary, based on the results, the multifractal singularity technique is robust and reliable since the results derived from are highly consistent with geological facts in the region and are most likely related to known copper mineralization areas. Finally, the normalized density index method was utilized to accurately define singularity based high favorable anomaly classes linked to magnetometric and radiometric data and also to generate binary anomaly and background maps. Thus, it can be used for similar investigations as well as additional large-scale studies in Sardouyeh region. In addition, integration of singularity based geophysical maps resulted in this research with other exploration data such as geological, geochemical and hydrothermal alterations data for generating mineral prospectivity models can be considered as the future topic for accurately highlighting the exploration targets.

Acknowledgements The authors would like to thank Prof. Babaie, the Editor-in-chief, for handling this manuscript. We also thank the anonymous reviewer for his/her constructive comments. Moreover, we want to thank the Geological Survey of Iran (GSI) for providing the geophysical database used in this paper.

Author contributions All authors contributed to the study conception and design. Data collection and modeling were performed by Sarina Akbari, Hamidreza Ramazi and Reza Ghezelbash. The first draft of the manuscript was written by Sarina Akbari. All authors read and approved the final manuscript.

Funding The authors did not receive support from any organization for the submitted work.

Data availability Not applicable.

Declarations

Conflict of interests The authors declare that they have no known competing financial interests or personal relationships that could have appeared to influence the work reported in this paper.

References

- Abedi M, Torabi SA, Norouzi GH, Hamzeh M (2012) ELECTRE III: A knowledge-driven method for integration of geophysical data with geological and geochemical data in mineral prospectivity mapping. *J Appl Geophys* 87:9–18
- Agterberg FP, Bonham-Carter GF (2005) Measuring the performance of mineral-potential maps. *Nat Resour Res* 14:1–17
- Agterberg FP, Cheng Q, Brown A, Good D (1996) Multifractal modeling of fractures in the Lac du Bonnet batholith, Manitoba. *Comput Geosci* 22(5):497–507
- Agterberg FP (2012) Multifractals and geostatistics. *J Geochem Explor* 122:113–122
- Akbari S, Ramazi H, Ghezelbash R, Maghsoudi A (2020) Geoelectrical integrated models for determining the geometry of karstic cavities in the Zarrinabad area, west of Iran: combination of fuzzy logic, CA fractal model and hybrid AHP-TOPSIS procedure. *Carbonates Evaporites* 35:1–16
- Ali MY, Fairhead JD, Green CM, Noufal A (2017) Basement structure of the United Arab Emirates derived from an analysis of regional gravity and aeromagnetic database. *Tectonophysics* 712:503–522
- Bai J, Porwal A, Hart C, Ford A, Yu L (2010) Mapping geochemical singularity using multifractal analysis: Application to anomaly definition on stream sediments data from Funin Sheet, Yunnan China. *J Geochem Explor* 104(1):1–11
- Baranov V (1957) A new method for interpretation of aeromagnetic maps: pseudogravimetric anomalies. *Geophysics* 22:359–383
- Baranov V, Naudy H (1964) Numerical calculation of the formula of reduction to the magnetic pole. *Geophysics* 29:67–79
- Bartier PM, Keller CP (1996) Multivariate interpolation to incorporate thematic surface data using inverse distance weighting (IDW). *Comput Geosci* 22(7):795–799
- Betts PG, Valenta RK, Finlay J (2003) Evolution of the Mount Woods Inlier, northern Gawler Craton, Southern Australia: an integrated structural and aeromagnetic analysis. *Tectonophysics* 366(1):83–111. [https://doi.org/10.1016/S0040-1951\(03\)00062-3](https://doi.org/10.1016/S0040-1951(03)00062-3)
- Bonham-Carter GF (1994) Geographical information systems for geoscientists: modeling with GIS. *Comput Methods Geosci* 13
- Carranza EJM, Zuo R, Cheng Q (2012) Fractal/multifractal modelling of geochemical exploration data. *J Geochem Explor* 122:1–3
- Carranza EJM (2008) Geochemical anomaly and mineral prospectivity mapping in GIS (vol. 11). Elsevier
- Carranza EJM (2009) Controls on mineral deposit occurrence inferred from analysis of their spatial pattern and spatial association with geological features. *Ore Geol Rev* 35(3):383–400
- Chen X, Xu R, Zheng Y, Jiang X, Du W (2018) Identifying potential Au-Pb-Ag mineralization in SE Shuangkoushan, North Qaidam, Western China: combined log-ratio approach and singularity mapping. *J Geochem Explor* 189:109–121
- Cheng Q (2007) Mapping singularities with stream sediment geochemical data for prediction of undiscovered mineral deposits in Gejiu, Yunnan Province, China. *Ore Geol Rev* 32(1–2):314–324

- Cheng Q (2008) Modeling local scaling properties for multiscale mapping. *Vadose Zone J* 7(2):525–532
- Cheng Q (2012) Singularity theory and methods for mapping geochemical anomalies caused by buried sources and for predicting undiscovered mineral deposits in covered areas. *J Geochem Explor* 122:55–70
- Cheng Q, Agterberg FP (2009) Singularity analysis of ore-mineral and toxic trace elements in stream sediments. *Comput Geosci* 35(2):234–244
- Cheng Q (1999) Spatial and scaling modelling for geochemical anomaly separation. *J Geochem Explor* 65(3):175–194
- Cheng Q, Agterberg FP, Ballantyne SB (1994) The separation of geochemical anomalies from background by fractal methods. *J Geochem Explor* 51(2):109–130
- Cheng Q, Xia Q, Li W, Zhang S, Chen Z, Zuo R, Wang W (2010) Density/area power-law models for separating multi-scale anomalies of ore and toxic elements in stream sediments in Gejiu mineral district, Yunnan Province, China. *Biogeosciences* 7(10):3019–3025
- Cheng Q, Xu Y, Grunsky E (2000) Integrated spatial and spectrum method for geochemical anomaly separation. *Nat Resour Res* 9(1):43–52
- Cheng WL (2001) Spatio-temporal variations of sulphur dioxide patterns with wind conditions in central Taiwan. *Environ Monit Assess* 66(1):77–98
- Cooper GRJ (2003) Feature detection using sun shading. *Comput Geosci* 29:941–948
- Cordell L, Grauch VJS (1985) Mapping basement magnetization zones from aeromagnetic data in the San Juan Basin, New Mexico. In *The utility of regional gravity and magnetic anomaly maps* (pp. 181–197). Society of Exploration Geophysicists
- Daviran M, Maghsoudi A, Ghezelbash R, Pradhan B (2021) A new strategy for spatial predictive mapping of mineral prospectivity: Automated hyperparameter tuning of random forest approach. *Comput Geosci* 148:104688
- Edwards DJ, Lyatsky HV, Brown RJ (1998) Regional interpretation of steep faults in the Alberta Basin from public-domain gravity and magnetic data: an update. *Can Soc Explor Geophys* 23(1):15–24
- Fedi M, Florio G (2001) Detection of potential fields source boundaries by enhanced horizontal derivative method. *Geophys Prospect* 49(1):40–58
- Ferdows MS, Ramazi H (2015a) Application of the fractal method to determine the membership function parameter for geoelectrical data (case study: Hamyj copper deposit, Iran). *J Geophys Eng* 12(6):909–921
- Ferdows MS, Ramazi H (2016) Performing the power spectrum-area method to separate anomaly from background for induced polarization data:(a case study; Hamyj copper deposit, Iran). *Arab J Geosci* 9(10):1–8
- Ferdows MS, Ramazi HR (2015b) Application of the singularity mapping technique to identify local anomalies by polarization data (a case study: Hamyj Copper Deposit, Iran). *Acta Geod Geoph* 50(3):365–374
- Forson ED, Menyeh A, Wemegah DD (2021) Mapping lithological units, structural lineaments and alteration zones in the Southern Kibi-Winneba belt of Ghana using integrated geophysical and remote sensing datasets. *Ore Geol Rev* 137:104271
- Ghezelbash R, Maghsoudi A (2018a) Comparison of U-spatial statistics and C-A fractal models for delineating anomaly patterns of porphyry-type Cu geochemical signatures in the Varzaghan district, NW Iran. *Compt Rendus Geosci* 350(4):180–191
- Ghezelbash R, Maghsoudi A (2018b) A hybrid AHP-VIKOR approach for prospectivity modeling of porphyry Cu deposits in the Varzaghan District, NW Iran. *Arab J Geosci* 11(11):275
- Ghezelbash R, Maghsoudi A, Carranza EJM (2019a) An improved data-driven multiple criteria decision-making procedure for spatial modeling of mineral prospectivity: adaption of prediction-area plot and logistic functions. *Nat Resour Res* 28(4):1299–1316
- Ghezelbash R, Maghsoudi A, Carranza EJM (2019b) Performance evaluation of RBF-and SVM-based machine learning algorithms for predictive mineral prospectivity modeling: integration of SA multifractal model and mineralization controls. *Earth Sci Inf* 12(3):277–293
- Ghezelbash R, Maghsoudi A, Carranza EJM (2020) Sensitivity analysis of prospectivity modeling to evidence maps: Enhancing success of targeting for epithermal gold, Takab district, NW Iran. *Ore Geol Rev* 120:103394
- Ghezelbash R, Maghsoudi A, Daviran M (2019c) Combination of multifractal geostatistical interpolation and spectrum-area (S-A) fractal model for Cu–Au geochemical prospects in Feizabad district, NE Iran. *Arab J Geosci* 12(5):1–14
- Ghezelbash R, Maghsoudi A, Shamekhi M, Pradhan B, Daviran M (2022) Genetic algorithm to optimize the SVM and K-means algorithms for mapping of mineral prospectivity. *Neural Comput Applic* 1–15
- Ghezelbash R, Daviran M, Maghsoudi A, Ghaeminejad H, Niknezhad M (2023) Incorporating the genetic and firefly optimization algorithms into K-means clustering method for detection of porphyry and skarn Cu-related geochemical footprints in Baft district, Kerman, Iran. *Appl Geochem* 148:105538
- Gonçalves BF, Sampaio EE (2013) Interpretation of airborne and ground magnetic and gamma-ray spectrometry data in prospecting for base metals in the central-north part of the Itabuna-Salvador-Curaçá Block, Bahia, Brazil Interpretation of Mag-Gama data. *Interpretation* 1(1):T85–T100
- Goncalves MA, Mateus A, Oliveira V (2001) Geochemical anomaly separation by multifractal modelling. *J Geochem Explor* 72(2):91–114
- Guan ZN (2005) *Geomagnetic field and magnetic exploration*. Geological Publishing House, Beijing
- Gunn PJ, Dentith MC (1997) Magnetic responses associated with mineral deposits. *J Aust Geol Geophys* 17:145–158
- Guo S, Lu YH, Zhang L, Zhang H (2008) Study on Fuzhou land price gradient field based on GIS. *J Lanzhou Univ* 44:33–38 ((in Chinese with English abstract))
- José-Ma M, Beatriz L (2006) Estimating housing price: Kriging the mean. *Int Adv Econ Res* 12:419
- Karim A, Mohamed H (2008) Regional-scale aeromagnetic survey of the south-west of Algeria: A tool for area selection for diamond exploration. *J Afr Earth Sci* 50:67–78
- Kalantari M, Ghezelbash S, Ghezelbash R, Yaghmaei B (2020) Developing a fractal model for spatial mapping of crime hot-spots. *Eur J Crim Policy Res* 26:571–591
- Li C, Ma T, Shi J (2003) Application of a fractal method relating concentrations and distances for separation of geochemical anomalies from background. *J Geochem Explor* 77(2–3):167–175
- Lima A, De Vivo B, Cicchella D, Cortini M, Albanese S (2003) Multifractal IDW interpolation and fractal filtering method in environmental studies: an application on regional stream sediments of (Italy), Campania region. *Appl Geochem* 18(12):1853–1865
- Liu Y, Cheng Q, Xia Q, Wang X (2013) Application of singularity analysis for mineral potential identification using geochemical data—A case study: Nanling W-Sn–Mo polymetallic metallogenic belt, South China. *J Geochem Explor* 134:61–72
- Liu Y, Xia Q, Cheng Q (2021) Aeromagnetic and geochemical signatures in the Chinese Western Tianshan: Implications for tectonic setting and mineral exploration. *Nat Resour Res* 30(5):3165–3195
- Mandelbrot BB (1983) *The fractal geometry of nature* (vol. 173). Macmillan
- Miller HG, Singh V (1994) Potential field tilt—a new concept for location of potential field sources. *J Appl Geophys* 32(2–3):213–217
- Rodriguez-Galiano V, Sanchez-Castillo M, Chica-Olmo M, Chica-Rivas MJOGR (2015) Machine learning predictive models for

- mineral prospectivity: An evaluation of neural networks, random forest, regression trees and support vector machines. *Ore Geol Rev* 71:804–818
- Sabzehie M, Afrooz A (1990) An analysis of lead and zinc mineralization in Dehaj-Sarduiye volcanic belt
- Akbari S, Ramazi H (2023) Application of AHP -SWOT and geophysical methods to develop a reasonable planning for Zagheh tourist destination considering environmental criteria. *Int J Environ Sci* 8:11–56
- Sun C, Liu G, Xue S (2016) Natural succession of grassland on the Loess Plateau of China affects multifractal characteristics of soil particle-size distribution and soil nutrients. *Ecol Res* 31(6):891–902
- Sun T, Li H, Wu K, Chen F, Zhu Z, Hu Z (2020) Data-driven predictive modelling of mineral prospectivity using machine learning and deep learning methods: a case study from southern Jiangxi Province, China. *Minerals* 10(2):102
- Sun X, Barros AP (2010) An evaluation of the statistics of rainfall extremes in rain gauge observations, and satellite-based and reanalysis products using universal multifractals. *J Hydrometeorol* 11(2):388–404
- Telford WM, Geldart LP, Sheriff RE, Keys DA (1976) *Applied Geophysics*. Cambridge University Press
- Uwiduhaye JDA, Mizunaga H, Saibi H (2018) Geophysical investigation using gravity data in Kinigi geothermal field, northwest Rwanda. *J Afr Earth Sc* 139:184–192
- Valenta RK, Jessell MW, Jung G, Bartlett J (1992) Geophysical interpretation and modelling of three-dimensional structure in the Duchess area, Mount Isa, Australia. *Explor Geophys* 23(2):393–400
- Verduzco B, Fairhead JD, Green CM, MacKenzie C (2004) New insights into magnetic derivatives for structural mapping. *Lead Edge* 23(2):116–119
- Wang F, Liao GP, Zhou XY, Shi W (2013) Multifractal detrended cross-correlation analysis for power markets. *Nonlinear Dyn* 72(1):353–363
- Wang J, Meng X (2019) An aeromagnetic investigation of the Dapai deposit in Fujian Province, South China: Structural and mining implications. *Ore Geol Rev* 112:103061
- Wang J, Zuo R (2018) Identification of geochemical anomalies through combined sequential Gaussian simulation and grid-based local singularity analysis. *Comput Geosci* 118:52–64
- Wang W, Zhao J, Cheng Q, Liu J (2012) Tectonic–geochemical exploration modeling for characterizing geo-anomalies in southeastern Yunnan district, China. *J Geochem Explor* 122:71–80
- Wang Z, Zuo R (2022) Mineral prospectivity mapping using a joint singularity-based weighting method and long short-term memory network. *Comput Geosci* 158:104974
- Wijns C, Perez C, Kowalczyk P (2005) Theta map: Edge detection in magnetic data. *Geophysics* 70(4):L39–L43
- William JH, Ralph RBVF, Saad AH (2013) *Gravity and Magnetic Exploration: Principles*. Cambridge University Press, New York, Practices and Applications
- Wu YZ (2005) GIS-based exploratory data analysis on the spatial–temporal evolvement of urban housing price and its application. Ph.D. dissertation thesis. Zhejiang Univ. pp 150 (in Chinese with English abstract)
- Xiao F, Chen J, Zhang Z, Wang C, Wu G, Agterberg FP (2012) Singularity mapping and spatially weighted principal component analysis to identify geochemical anomalies associated with Ag and Pb-Zn polymetallic mineralization in Northwest Zhejiang, China. *J Geochem Explor* 122:90–100
- Yang N, Zhang Z, Yang J, Hong Z, Shi J (2021) A convolutional neural network of GoogLeNet applied in mineral prospectivity prediction based on multi-source geoinformation. *Nat Resour Res* 30(6):3905–3923
- Yuan F, Li X, Zhou T, Deng Y, Zhang D, Xu C, Zhang R, Jia C, Jowitz SM (2015) Multifractal modelling-based mapping and identification of geochemical anomalies associated with Cu and Au mineralisation in the NW Junggar area of northern Xinjiang Province, China. *J Geochem Explor* 154:252–264
- Zhang P, Du J, Wang Z, Yang M, Chen C (2022) Extraction, evaluation and replacement techniques of long wavelength components from compiled regional aeromagnetic anomaly data. *Chin J Geophys* 7:2595–2612
- Zhao J, Chen S, Zuo R (2016) Identifying geochemical anomalies associated with Au–Cu mineralization using multifractal and artificial neural network models in the Ningqiang district, Shaanxi, China. *J Geochem Explor* 164:54–64
- Zuo R, Wang J (2016) Fractal/multifractal modeling of geochemical data: a review. *J Geochem Explor* 164:33–41

Publisher's note Springer Nature remains neutral with regard to jurisdictional claims in published maps and institutional affiliations.

Springer Nature or its licensor (e.g. a society or other partner) holds exclusive rights to this article under a publishing agreement with the author(s) or other rightsholder(s); author self-archiving of the accepted manuscript version of this article is solely governed by the terms of such publishing agreement and applicable law.